

IMPROVING PRIVACY-PRESERVING VERTICAL FEDERATED LEARNING BY EFFICIENT COMMUNICATION WITH ADMM

Chulin Xie¹, Pin-Yu Chen², Ce Zhang³, Bo Li¹

¹University of Illinois Urbana-Champaign, ²IBM Research, ³ETH Zurich

ABSTRACT

Federated learning (FL) enables an effective framework for distributed resource-constrained devices such as mobile phones to jointly train a shared model while keeping the training data local for privacy purposes. Different from the horizontal FL (HFL) setting where each client has partial data samples, vertical FL (VFL), which allows each client to collect partial features, has attracted intensive research efforts recently. In this paper, we identified two challenges that state-of-the-art VFL frameworks are facing: (1) some works directly average the learned feature embeddings and therefore might lose the unique properties of each local feature set; (2) server needs to communicate gradients with the clients for *each* training step, incurring high communication cost that leads to rapid consumption of privacy budgets. In this paper, we aim to address the above challenges and propose an efficient VFL with multiple linear heads (VIM) framework, where each linear head corresponds to local clients by taking the separate contribution of each client into account. In addition, we propose an Alternating Direction Method of Multipliers (ADMM)-based method to solve our optimization problem, which reduces the communication cost by allowing multiple local updates in each step, and thus leads to better performance under differential privacy. We consider various settings including VFL with model splitting (i.e., clients host partial models) and without model splitting (i.e., clients host the entire model). For both settings, we carefully analyze the differential privacy mechanism for our framework. Moreover, we show that a byproduct of our framework is that the weights of learned linear heads reflect the importance of local clients. We conduct extensive evaluations and show that on four real-world datasets, VIM achieves significantly higher performance and faster convergence compared with state-of-the-arts. We also explicitly evaluate the importance of local clients and show that VIM enables functionalities such as client-level explanation and client denoising. We hope this work will shed light on a new way of effective VFL training and understanding.

1 INTRODUCTION

Federated learning (FL) has enabled large-scale training with data privacy guarantees on distributed data for different applications (Yang et al., 2019c; Brisimi et al., 2018; Hard et al., 2018; Yang et al., 2018; 2019a). In general, FL can be categorized into Horizontal FL (HFL) (McMahan et al., 2017) where data samples are distributed across clients, and Vertical FL (VFL) (Yang et al., 2019a) where features of the samples are partitioned across clients and the labels are usually owned by the server (or the active party in two-party setting (Hardy et al., 2017)). In particular, VFL allows agents with partial information of the same dataset to jointly train the model, which leads to many real-world applications (Hu et al., 2019b; Yang et al., 2019a; Hard et al., 2018). For instance, a patient may go to different types of clinics such as dental clinics and pharmacies for different purposes, and therefore it is important for different clinics to “share” their information about the same patient to better model the health condition of the patient. In addition, multimodal data has been ubiquitous currently, while usually each agent is only able to collect one or a few data modality due to resource limitations, and therefore the VFL framework provides an effective way to allow such agents to jointly train a model leveraging information from different data modalities.

Despite the importance and practicality of VFL, there are mainly two weaknesses of the state-of-the-art (SOTA) VFL frameworks: (1) some VFL frameworks directly average the feature embeddings from local agents, and therefore fail to capture the unique properties of each local feature set (Chen et al., 2020); (2) the server usually needs to send gradients to clients for *each* training step which leads to high communication cost and potentially rapid consumption of privacy budget (Chen et al., 2020; Hu et al., 2019b; Kang et al., 2020).

To solve the above challenges, in this work, we propose an efficient VFL optimization framework with multiple linear heads (VIM), where each linear head corresponds to one local client, taking the individual contribution of clients into consideration and thereby improving the overall performance. In particular, we propose an Alternating Direction Method of Multipliers (ADMM) (Boyd et al., 2011)-based method to solve our optimization problem, which allows multiple local updates in each step, thus yielding faster convergences and reducing the communication cost. This is critical to preserving privacy since the privacy costs increases as the number of communication rounds increases (Abadi et al., 2016). We consider various VFL settings including *with model splitting* (i.e., clients host partial models) and *without model splitting* (i.e., clients hold the entire model). Under the with model splitting setting, we propose the gradient-based algorithm $VIMSGD$ as well as the ADMM-based algorithm $VIMADMM$ under VIM framework. Compared to gradient-based methods, $VIMADMM$ not only reduces communication frequency but also reduces the dimensionality by only exchanging ADMM-related variables. With modifications of communication strategies and updating rules for servers and clients, we extend $VIMADMM$ to the without model splitting setting and propose $VIMADMM-J$. Under both settings, to further protect the privacy of local data, we propose to clip and perturb local outputs to satisfy differential privacy (DP) (Dwork et al., 2006; Dwork, 2011; Dwork & Roth, 2014) and prove the DP guarantees for VIM. Moreover, we show that a byproduct of VIM is that the weights of learned linear heads reflect the importance of local clients, which enables functionalities such as client-level explanation, client denoising, and client summarization. Our main technical contributions are:

- We propose an efficient and effective VFL optimization framework with multiple linear heads (VIM). To solve our optimization problem, we propose an ADMM-based method, which reduces communication costs by allowing multiple local updates at each step.
- We propose the DP mechanism for our VIM framework and prove its privacy guarantees.
- We conduct extensive experiments on MNIST, CIFAR, NUS-WIDE, and ModelNet40 datasets, and show that ADMM-based algorithms under VIM converge faster, achieve higher accuracy, and remain higher utility under DP than existing VFL frameworks.
- We evaluate our client-level explanation under VIM based on the linear heads weights norm, and demonstrate the functionalities it enables such as clients denoising and summarization.

2 RELATED WORK

Vertical Federated Learning. VFL has been well studied for simple models including trees (Cheng et al., 2021; Wu et al., 2020), kernel models (Gu et al., 2020), and linear and logistic regression (Hardy et al., 2017; Yang et al., 2019b; Zhang et al., 2021; Feng & Yu, 2020; Hu et al., 2019a; Liu et al., 2019). For DNNs, there are two popular VFL settings: with model splitting (Vepakomma et al., 2018;?; Chen et al., 2020) and without model splitting (Hu et al., 2019b; Jin et al., 2021). In the model splitting setting, split learning (Vepakomma et al., 2018) is the first related paradigm, where each client trains a partial network up to a cut layer, the server concatenates local activations and trains the rest of the network. However, despite its promising performance in HFL, it was not evaluated on vertically partitioned data. VAFL (Chen et al., 2020) is proposed for VFL where the server averages the local embeddings and sends gradients back to clients to update local models. However, such embedding averaging might lose the unique properties of each client. FedMVT (Kang et al., 2020) focuses on the semi-supervised VFL with multi-view learning. For VFL without model splitting setting, in FDML (Hu et al., 2019b) framework, each client submits local logits to the server, who averages over the logits and send gradients back to clients. We note that all SOTA methods (Chen et al., 2020; Kang et al., 2020; Hu et al., 2019b) require the communication of gradients at *each* training step, leading to high communication costs before convergence.

Differentially Private VFL. In this work, we focus on the standard privacy notion (ϵ, δ) -DP (Dwork et al., 2006; Dwork, 2011; Dwork & Roth, 2014). In existing VFL frameworks,

VAFL (Chen et al., 2020) provides Gaussian DP guarantee (Dong et al., 2019), which is less practical than (ϵ, δ) -DP; FDML (Hu et al., 2019b) evaluate their framework under different levels of empirical noises, yet without offering detailed DP mechanisms or (ϵ, δ) -DP guarantee; the ADMM-based framework (Hu et al., 2019a) provides (ϵ, δ) -DP guarantee for linear models by calculating the closed-form sensitivity of each sample and perturbing the linear model parameters, which is not directly applicable to DNNs whose sensitivity is hard to estimate due to the nonconvexity. Instead, we propose to perturb local outputs and provide formal (ϵ, δ) -DP theoretical guarantee in Section 4.

3 VFL WITH MULTIPLE LINEAR HEADS (VIM)

3.1 FRAMEWORK OVERVIEW

In VFL, we have M clients $\{1, 2, \dots, M\}$ who hold different feature sets of the same training samples to jointly train a machine learning model. We consider the classification task and denote d_c as the number of classes. Suppose there is a training dataset $D = \{x_j, y_j\}_{j=1}^N$ containing N samples, the server owns the labels $\{y_j\}_{j=1}^N$, and each client k has a local feature set $X_k = \{x_j^k\}_{j=1}^N$, where the vector $x_j^k \in \mathbb{R}^{d^k}$ denotes the local (partial) features of sample j . The overall feature $x_j \in \mathbb{R}^d$ of sample j is the concatenation of all local features $\{x_j^1, x_j^2, \dots, x_j^M\}$, with $d = \sum_{k=1}^M d^k$.

Due to the privacy protection requirement of VFL, each client k does not share raw local feature set X_k with other clients or the server. Instead, VFL consists of two steps: (1) *local processing step*: each client learns a local model that maps the local features to local outputs and sends them to the server. (2) *server aggregation step*: the server aggregates the local outputs from all clients to compute the final prediction for each sample as well as the corresponding losses. Depending on whether or not the server holds a model, there are two popular VFL settings (Fu et al., 2022): *VFL with model splitting* (Chen et al., 2020; Vepakomma et al., 2018) and *VFL without model splitting* (Hu et al., 2019b): (i) In the model splitting setting, each client trains a feature extractor as the local model that outputs *local embeddings*, and the server owns a model which predicts the final results based on the aggregated embeddings. (ii) In the VFL without model splitting setting, the clients host the entire model that outputs the *local logits*, and the server simply performs the logits aggregation operation without hosting any model.

In both settings, the local model is updated by federated backward propagation (Fu et al., 2022): a) the server first computes the gradients of the loss w.r.t the local output (either embeddings or logits) from each client separately and sends the gradients back to clients; b) each client calculates the gradients of local output w.r.t the local model parameters and updates the local model using the chain rule.

We will first dive into the details of the model splitting setting and introduce our framework VIM as well as the corresponding SGD-based method VIMSGD and ADMM-based method VIMADMM. Then, we will show that our ADMM-based method can be easily extended to the VFL without model splitting setting with slight modifications, which is based on different communication strategies and update rules for server and clients, yielding the method VIMADMM-J.

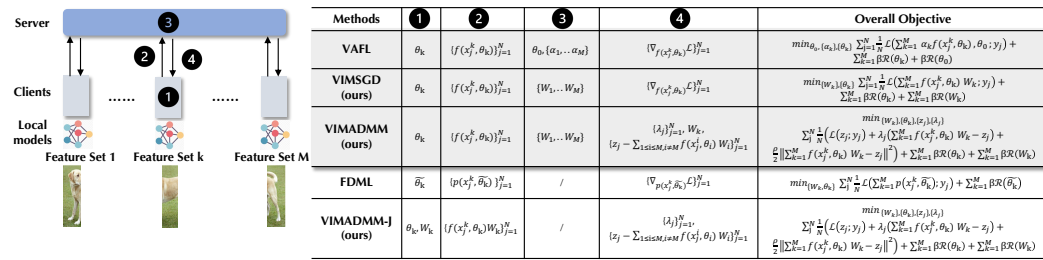


Figure 1: Overview of different Vertical FL methods. Grey background here represents the *VFL with model splitting* setting, and white background represents *VFL without model splitting* setting.

3.2 VFL WITH MODEL SPLITTING

Setup. Let f parameterized by θ_k be the local model (i.e., feature extractor) of client k , which outputs a local embedding vector $h_j^k = f(x_j^k, \theta_k) \in \mathbb{R}^{d_f}$ for each local feature x_j^k . We denote the parameters of the model on the server-side as θ_0 . Overall, the clients and the server aim to collaboratively solve the Empirical Risk Minimization (ERM) objective:

$$\min_{\{\theta_k\}_{k=1}^M, \theta_0} \sum_{j=1}^N \ell(h_j^1, \dots, h_j^M, \theta_0; y_j) + \sum_{k=1}^M \beta \mathcal{R}(\theta_k) + \beta \mathcal{R}(\theta_0) \quad \text{with } h_j^k = f(x_j^k, \theta_k), \forall k \in [M], \quad (1)$$

where ℓ is a loss function (e.g., cross-entropy loss with softmax function), \mathcal{R} is a regularizer on model parameters, and $\beta \in \mathbb{R}$ is the regularization weight for client k or the server. We consider \mathcal{R} to be differentiable but are optimistic that it can be extended to other regularizers as future work. In principle, β can be different for different models, and we use the same β here for simplicity.

VIM Formulation. We start by noting that for the server aggregation step, the SOTA method, VAFL (Chen et al., 2020), directly averages the local embeddings $\sum_{k=1}^M \alpha_k h_j^k$ where the scalar $\alpha_k \in \mathbb{R}$ is the aggregation weight for client k and it can be optimized during training as an additional parameter in the ERM loss. Therefore, the objective function of VAFL is $\min_{\{\theta_k\}_{k=1}^M, \{\alpha_k\}_{k=1}^M, \theta_0} \sum_{j=1}^N \ell(\sum_{k=1}^M \alpha_k h_j^k, \theta_0; y_j) + \sum_{k=1}^M \beta \mathcal{R}(\theta_k) + \beta \mathcal{R}(\theta_0)$. However, such an aggregation implicitly assumes that each dimension of the embedding vectors from different clients shares the same contextual meaning in the latent space so that they can be directly averaged. Such a design may be suboptimal, since in VFL different local embeddings can represent different aspects of the same sample, and therefore average-based aggregation might lose the unique properties of each local feature set.

To address the above average-based aggregation problem, we propose VIM, a novel VFL framework where the server learns a model with multiple linear heads corresponding to local clients, taking the separate contribution of each client into account. Specifically, the server’s model θ_0 consists of M linear heads W_1, W_2, \dots, W_M with $W_k \in \mathbb{R}^{d_f \times d_c}$, $k \in [M]$, and the server’s model outputs $\sum_{k=1}^M h_j^k W_k$ as the prediction for sample j , yielding our VIM objective:

$$\min_{\{W_k\}_{k=1}^M, \{\theta_k\}_{k=1}^M} \mathcal{L}_{\text{VIM}}(\{W_k\}_{k=1}^M, \{\theta_k\}_{k=1}^M) := \sum_{j=1}^N \ell(\sum_{k=1}^M h_j^k W_k; y_j) + \sum_{k=1}^M \beta \mathcal{R}(\theta_k) + \sum_{k=1}^M \beta \mathcal{R}(W_k) \quad (2)$$

Despite the simplicity of linear heads, recent studies in representation learning show that the linear classifier is an efficient approach to predicting the labels on top of embedding representations (Radford et al., 2021; Khosla et al., 2020), given the expressive power of the local feature extractor which captures essential information from raw feature sets.

VIMSGD. In practice, existing VFL frameworks often use stochastic gradient descent (SGD) to alternatively update the server’s model and local models (Chen et al., 2020; Kang et al., 2020) where the clients send a *batch* of embeddings to the server, and the server sends a *batch* of gradients to clients at each communication round. We provide the SGD-based algorithm VIMSGD under the VIM framework (The Algorithm 2 and detailed description are deferred to Appendix A), which serves as a strong baseline.

VIMADMM. The SGD-based methods including the state-of-art VAFL require the server to send the *gradients* w.r.t embeddings back to clients at *every* training step of the local models. However, such (1) frequent communication and (2) the high dimensionality of gradients (i.e., bd_f for b samples) lead to high communication costs. To address the above limitations, we propose an ADMM-based method for VIM, reducing the communication frequency by allowing multiple local updates at each round, and reducing the dimensionality by only exchanging ADMM-related variables (i.e., $(2b + d_f)d_c$ for b samples where $d_c \ll d_f, b$ for most VFL settings today (Chen et al., 2020; Hu et al., 2019b)). Specifically, the multiple linear heads in VIM enable the application of ADMM via a special decomposition into simpler sub-problems that can be solved in a distributed manner. We begin by

rewriting Eq. 2 to an equivalent constrained optimization problem:

$$\min_{\{W_k\}_{k=1}^M, \{\theta_k\}_{k=1}^M, \{z_j\}_{j=1}^N} \sum_{j=1}^N \ell(z_j; y_j) + \beta \sum_{k=1}^M (\mathcal{R}(\theta_k) + \mathcal{R}(W_k)) \quad \text{s.t.} \quad \sum_{k=1}^M h_j^k W_k - z_j = 0, \forall j \in [N] \quad (3)$$

where $z_1, z_2, \dots, z_N \in \mathbb{R}^{d_c}$ are auxiliary variables. Each constraint implies a consensus between the server's output $\sum_{k=1}^M h_j^k W_k$ and the auxiliary variable z_j for the sample j . To solve Eq. 3, we define the augmented Lagrangian (Boyd et al., 2011) which adds a quadratic term to Lagrangian as:

$$\min_{\{W_k\}_{k=1}^M, \{\theta_k\}_{k=1}^M, \{z_j\}_{j=1}^N, \{\lambda_j\}_{j=1}^N} \mathcal{L}(\{W_k\}_{k=1}^M, \{\theta_k\}_{k=1}^M, \{z_j\}_{j=1}^N, \{\lambda_j\}_{j=1}^N) := \sum_{j=1}^N \ell(z_j; y_j) + \beta \sum_{k=1}^M (\mathcal{R}(\theta_k) + \mathcal{R}(W_k)) + \sum_{j=1}^N \lambda_j^\top \left(\sum_{k=1}^M h_j^k W_k - z_j \right) + \frac{\rho}{2} \sum_{j=1}^N \left\| \sum_{k=1}^M h_j^k W_k - z_j \right\|_F^2, \quad (4)$$

where $\lambda_j \in \mathbb{R}^{d_c}$ is the dual variable for sample j , and $\rho \in \mathbb{R}^+$ is a constant penalty factor. To solve Eq. 4, we follow the standard ADMM algorithm (Boyd et al., 2011) and update the primal variables $\{W_k\}$, $\{\theta_k\}$, $\{z_j\}$ and the dual variables $\{\lambda_j\}$ *alternatively* as follows:

$$\begin{aligned} W_k^{(t+1)} &= \underset{W_k}{\operatorname{argmin}} \mathcal{L}(\{\theta_k^{(t)}\}, W_k, \{z_j^{(t)}\}, \{\lambda_j^{(t)}\}), \forall k \in [M], \\ \theta_k^{(t+1)} &= \underset{\theta_k}{\operatorname{argmin}} \mathcal{L}(\theta_k, \{W_k^{(t+1)}\}, \{z_j^{(t)}\}, \{\lambda_j^{(t)}\}), \forall k \in [M], \\ z_j^{(t+1)} &= \underset{z_j}{\operatorname{argmin}} \mathcal{L}(\{\theta_k^{(t+1)}\}, \{W_k^{(t+1)}\}, z_j, \{\lambda_j^{(t)}\}), \forall j \in [N], \\ \lambda_j^{(t+1)} &= \underset{\lambda_j}{\operatorname{argmin}} \mathcal{L}(\{\theta_k^{(t+1)}\}, \{W_k^{(t+1)}\}, \{z_j^{(t+1)}\}, \lambda_j), \forall j \in [N], \end{aligned} \quad (5)$$

which decomposes the problem in Eq. 3 into four sets of sub-problems over $\{W_k\}$, $\{\theta_k\}$, $\{z_j\}$, $\{\lambda_j\}$, and each sub-problem can be solved *in parallel*. In practice, we propose the following strategy for the alternative updating in the server and clients: (i) updating $\{z_j\}$, $\{\lambda_j\}$ and $\{W_k\}$ at server-side, (ii) updating $\{\theta_k\}$ at the client-side in parallel. Moreover, we consider the realistic setting of stochastic ADMM with mini-batches. Concretely, at communication round t , the server samples a set of data indices, $B(t)$, with batch size $|B(t)| = b$. Then we describe the key steps of VIMADMM as follows:

(1) Communication from client to server. Each client k sends a batch of embeddings $\{h_j^k\}_{j \in B(t)}$ to the server, where $h_j^k = f(x_j^k, \theta_k^{(t)})$, $\forall j \in B(t)$.

(2) Sever updates auxiliary variables $\{z_j\}$. After receiving the local embeddings from all clients, the server updates the auxiliary variable for each sample j as:

$$z_j^{(t+1)} = \underset{z_j}{\operatorname{argmin}} \ell(z_j; y_j) - \lambda_j^{(t)\top} z_j + \frac{\rho}{2} \left\| \sum_{k=1}^M h_j^k W_k^{(t)} - z_j \right\|_F^2, \forall j \in B(t) \quad (6)$$

Since the optimization problem in Eq. 6 is convex and differentiable with respect to z_j , we use the L-BFGS-B algorithm (Zhu et al., 1997) to solve the minimization problem.

(3) Sever updates dual variables $\{\lambda_j\}$. After the updates in Eq. 6, the server updates the dual variable for each sample j as:

$$\lambda_j^{(t+1)} = \lambda_j^{(t)} + \rho \left(\sum_{k=1}^M h_j^k W_k^{(t)} - z_j^{(t+1)} \right), \forall j \in B(t) \quad (7)$$

(4) Sever updates linear heads $\{W_k\}$. After the updates in Eq. 7, each linear head of the server is then updated as:

$$W_k^{(t+1)} = \underset{W_k}{\operatorname{argmin}} \beta \mathcal{R}(W_k) + \sum_{j \in B(t)} \lambda_j^{(t+1)\top} h_j^k W_k + \sum_{j \in B(t)} \frac{\rho}{2} \left\| \sum_{i \in [M], i \neq k} h_j^i W_i^{(t)} + h_j^k W_k - z_j^{(t+1)} \right\|_F^2, \forall k \in [M] \quad (8)$$

Algorithm 1: VIMADMM (Changes for differential privacy highlighted in gray)

Input: number of communication rounds T , number of clients M , number of training samples N , batch size b , input features $\{\{x_j^1\}_{j=1}^N, \{x_j^2\}_{j=1}^N, \dots, \{x_j^M\}_{j=1}^N\}$, the labels $\{y_j\}_{j=1}^N$, local model $\{\theta_k\}_{k=1}^M$; linear heads $\{W_k\}_{k=1}^M$; auxiliary variables $\{z_j\}_{j=1}^N$; dual variables $\{\lambda_j\}_{j=1}^N$; noise parameter σ , clipping constant C

- 1 **for** communication round $t \in [T]$ **do**
- 2 Server samples a set of data indices $B(t)$ with $|B(t)| = b$
- 3 **for** client $k \in [M]$ **do**
- 4 **generates** a local training batch $\{x_j^k\}_{j \in B(t)}$
- 5 **computes** local embeddings $h_j^{k(t)} \leftarrow f(x_j^k, \theta_k), \forall j \in B(t)$
- 6 **clips and perturbs** local embeddings $h_j^{k(t)} \leftarrow \text{Clip}(h_j^{k(t)}, C) + \mathcal{N}(0, \sigma^2 C^2), \forall j \in B(t)$
- 7 **sends** local embeddings $\{h_j^{k(t)}\}_{j \in B(t)}$ to the server
- 7 Server **updates** auxiliary variables $z_j^{(t+1)}$ via Eq. 6, $\forall j \in B(t)$
- 8 Server **updates** dual variables $\lambda_j^{(t+1)}$ via Eq. 7, $\forall j \in B(t)$
- 9 Server **updates** linear heads $W_k^{(t+1)}$ with objective of Eq. 8, $\forall k \in [M]$
- 10 Server **computes** residual variables $s_j^{k(t+1)}$ via Eq. 9, $\forall j \in B(t), k \in [M]$
- 11 Server **sends** $\{\lambda_j^{(t+1)}\}_{j \in B(t)}, \{s_j^{k(t+1)}\}_{j \in B(t)}$ and corresponding $W_k^{(t+1)}$ to each client $k, \forall k \in [M]$
- 12 **for** client $k \in [M]$ **do**
- 13 **for** local step $e \in [\tau]$ **do**
- 14 **updates** local model $\theta_k^{(t+1)}$ via SGD with objective of Eq. 10

For squared ℓ_2 regularizer \mathcal{R} , we can solve $W_k^{(t+1)}$ in an inexact way to save the computation by *one* step of SGD with the objective of Eq. 8.

(5) Communication from server to client. After the updates in Eq. 8, we define a residual variable $s_j^{k(t+1)}$ for each sample j of k -th client, which provides supervision for updating local model:

$$s_j^{k(t+1)} \triangleq z_j^{(t+1)} - \sum_{i \in [M], i \neq k} h_j^{i(t)} W_i^{(t+1)}, \forall j \in B(t), \forall k \in [M] \quad (9)$$

The server sends the dual variables $\{\lambda_j^{(t+1)}\}_{j \in B(t)}$ and the residual variables $\{s_j^{k(t+1)}\}_{j \in B(t)}$ of all samples, as well as the *corresponding* linear head $W_k^{(t+1)}$ to each client k .

(6) Client updates local model parameters θ_k . Finally, every client k locally updates the model parameters θ_k as follows:

$$\theta_k^{(t+1)} = \underset{\theta_k}{\operatorname{argmin}} \quad \beta \mathcal{R}(\theta_k) + \sum_{j \in B(t)} \lambda_j^{(t+1)\top} f(x_j^k, \theta_k) W_k^{(t+1)} + \frac{\rho}{2} \sum_{j \in B(t)} \left\| s_j^{k(t+1)} - f(x_j^k, \theta_k) W_k^{(t+1)} \right\|_F^2 \quad (10)$$

Due to the nonconvexity of the loss function of DNN, we use τ local steps of SGD to update the local model at each round with the objective of Eq. 10. We note that multiple local updates of Eq. 10 enabled by ADMM lead to better local models at each communication round compared to gradient-based methods, thus VIMADMM requires fewer communication rounds to converge as we will show in Sec. 5.1. These six steps of VIMADMM are summarized in Algorithm 1.

Note that ADMM auxiliary variables $\{z_j\}$ and dual variables $\{\lambda_j\}$ are only used during the training time optimization process. Therefore, in the test phase, for any sample x_j , the server directly uses the trained multiple linear heads to make prediction $\sum_{k=1}^M h_j^k W_k$.

Remarks. There are several key challenges of deploying ADMM in VFL for distributed optimization: (1) how to ensure the consensus among clients and form it as a constrained optimization problem (e.g., Eq. 3); (2) how to decompose the optimization problem (i.e., the main objective function

in Eq. 3) into small sub-problems that can be solved in parallel by ADMM (e.g., Eq. 5). For the first challenge, although ADMM is flexible to introduce auxiliary variables and thus formulate a constrained optimization problem in HFL, it raises new challenges in VFL. For example, the ADMM-based methods in HFL (Elgabli et al., 2020b;a; Huang et al., 2019; Yue et al., 2021) usually use the global model as the auxiliary variable and enforce the consistency between the global model and each local model. However, VFL communicates embeddings, and it is not feasible to enforce local embeddings from different clients to be the same as they provide unique information from different aspects. Therefore, in this paper, we introduce the auxiliary variable z_j for each sample j and construct the constraint between z_j and server’s output $\sum_{k=1}^M h_j^k W_k$ (i.e., the logits), which enables the optimization for each W_k by ADMM (i.e., Eq. 5). For the second challenge, we propose the bi-level optimization for server’s model and clients’ models to train DNNs for VFL with model splitting, while the existing ADMM-based method in VFL (Hu et al., 2019a) only considers logistic regression with linear models in client-side, which does not apply to DNNs. The initial attempt we made is to decompose the optimization for server’s linear heads by ADMM while still using chain rule of SGD to update local models, which does not exhibit much superiority over pure SGD-based methods. Later, we decompose the optimization for both server’s linear heads and local models by ADMM, leading to our current algorithm VIMADMM that enables multiple local updates for clients at each communication round and achieves significantly better performance as we will show in Sec. 5.1.

3.3 VFL WITHOUT MODEL SPLITTING

Setup. Recall the VFL without model splitting setting described in Section 3.1. Let p parameterized by $\tilde{\theta}_k$ be the local model (i.e., whole model) of client k , which outputs local logits $o_j^k = p(x_j^k, \tilde{\theta}_k) \in \mathbb{R}^{d_c}$ for each local feature x_j^k . The clients and the server aim to jointly solve the problem: $\min_{\{\tilde{\theta}_k\}_{k=1}^M} \sum_{j=1}^N \ell(o_j^1, \dots, o_j^M; y_j) + \beta \sum_{k=1}^M \mathcal{R}(\tilde{\theta}_k)$ with $o_j^k = p(x_j^k, \tilde{\theta}_k), \forall k \in [M]$.

VIMADMM-J. In the state-of-art VFL framework FDML, the server averages the local logits as final prediction $\sum_{k=1}^M o_j^k$, and FDML also suffers from the high communication cost by sending the gradients w.r.t. local logits to each client at *each* training step of the local model. To solve this problem with our VIM framework, we adapt VIMADMM to the without model splitting setting and propose VIMADMM-J , where each linear head W_k is held by the corresponding client k , and is always updated locally. At each communication round t , VIMADMM-J does the following: **(1)** each client k sends local logits $\{o_j^k\}_{j \in B(t)}$ with $o_j^k = f(x_j^k, \theta_k^{(t)})W_k^{(t)}$ to the server; **(2)** the server updates the auxiliary variables $\{z_j^{(t+1)}\}_{j \in B(t)}$, dual variables $\{\lambda_j^{(t+1)}\}_{j \in B(t)}$, and computes residual variables $\{s_j^{k(t+1)}\}_{j \in B(t)}$; **(3)** the server sends updated dual variables $\{\lambda_j^{(t+1)}\}_{j \in B(t)}$, and residual variables $\{s_j^{k(t+1)}\}_{j \in B(t)}$ to each client k ; **(4)** each client k alternatively updates linear head $W_k^{(t+1)}$ and feature extractor $\theta_k^{(t+1)}$ with τ local steps of SGD. The detailed description of key steps of VIMADMM-J and the corresponding Algorithm 3 are presented in Appendix A.

4 DIFFERENTIALLY PRIVATE VIM

Although the raw features and local models are kept locally without sharing in VFL, sharing the model outputs such as latent representations or predictions during the training process might also leak sensitive user information (Papernot et al., 2018). Therefore, we aim to further protect the privacy of the local feature set X_k of each client k from the malicious server and other clients. We start by the definition of (ϵ, δ) -DP, which guarantees that the change in a randomized algorithm’s output distribution caused by a small input difference is bounded.

Definition 1 ((ϵ, δ) -DP (Dwork & Roth, 2014)). *A randomized algorithm $\mathcal{M} : \mathcal{X}^n \mapsto \Theta$ is (ϵ, δ) -DP if for every pair of neighboring datasets $X, X' \in \mathcal{X}^n$ (i.e., differing only by one data point), and every possible (measurable) output set $E \subseteq \Theta$ the following inequality holds: $\Pr[\mathcal{M}(X) \in E] \leq e^\epsilon \Pr[\mathcal{M}(X') \in E] + \delta$.*

Since the only shared information is the local outputs, we propose the following DP mechanisms to perturb the local outputs of each client k at every round t : (1) *clip* the per-sample local output (either

embedding $h_j^{k(t)}$ or logit $o_j^{k(t)}$ with threshold C such that its ℓ_2 -sensitivity is upper bounded by C (2) add *Gaussian noise* sampled from $\mathcal{N}(0, \sigma^2 C^2)$, which is proportional to C and can randomize the local output, i.e., $\text{Clip}\left(h_j^{k(t)}, C\right) + \mathcal{N}\left(0, \sigma^2 C^2\right)$ or $\text{Clip}\left(o_j^{k(t)}, C\right) + \mathcal{N}\left(0, \sigma^2 C^2\right), \forall j \in B(t), \forall k \in [M]$. Based on the above modification to our algorithms, we now provide the privacy guarantee for the DP version of Algorithm 1, 2, 3 in Theorem 1.

Theorem 1. *Given a local feature set with N samples, the subsampling ratio $\gamma = b/N$ without replacement, the number of communication rounds T , the clipping threshold C , the noise parameter σ , our DP version of Algorithm 1, 2, 3 satisfies $(T\epsilon'(\alpha) + \log \frac{\alpha-1}{\alpha} - \frac{\log \delta + \log \alpha}{\alpha-1}, \delta)$ -DP with $\epsilon(\alpha) = \alpha/(2\sigma^2)$ where,*

$$\begin{aligned} \epsilon'(\alpha) \leq & \frac{1}{\alpha-1} \log \left(1 + \gamma^2 \binom{\alpha}{2} \min \left\{ 4 \left(e^{\epsilon(2)} - 1 \right), e^{\epsilon(2)} \min \left\{ 2, \left(e^{\epsilon(\infty)} - 1 \right)^2 \right\} \right\} \right. \\ & \left. + \sum_{j=3}^{\alpha} \gamma^j \binom{\alpha}{j} e^{(j-1)\epsilon(j)} \min \left\{ 2, \left(e^{\epsilon(\infty)} - 1 \right)^j \right\} \right) \end{aligned} \quad (11)$$

Proof Sketch. We derive the theorem with Rényi Differential Privacy (RDP) (Mironov, 2017) as a bridge. We first leverage RDP guarantee for Gaussian mechanism (Mironov, 2017) to analyze the local output perturbation, and adopt RDP subsampling privacy amplification (Wang et al., 2019) to analyze the effect of mini-batch at each communication round. Then we use the RDP Composition theorem (Mironov, 2017) to accumulate the privacy budget over T communication rounds, and finally, convert RDP guarantee into DP guarantee (Balle et al., 2020). The detailed proof is given in Appendix C.

5 EXPERIMENTS

In this section, we conduct extensive experiments on four real-world datasets. We show that our proposed framework VIM achieves significantly faster convergence and higher accuracy than SOTA, maintains higher utility under DP, and enables client-level explainability.

Data and Models. We consider the classification task on four datasets: MNIST (LeCun & Cortes, 2010), CIFAR (Krizhevsky, 2009), NUS-WIDE (Chua et al., 2009), a multi-modality dataset with image features and textual features, and ModelNet40 (Su et al., 2018), a multi-view image dataset. As shown in Figure 5 row 1, we simulate VFL scenarios by splitting the data features to $\{14, 9, 4, 4\}$ clients for the four datasets respectively. As for the local model, we use a two-layer fully connected model for MNIST and NUS-WIDE, a CNN model for CIFAR, and ResNet-18 (He et al., 2016) for ModelNet40. To prevent over-fitting, we adopt standard stopping criteria, i.e., stop training when the model converges or the validation accuracy starts to drop more than 2%. We refer to Appendix B for more details about datasets, networks, and parameter selection.

Baselines. We compare VIMSGD, VIMADMM with VAFL (Chen et al., 2020) under *w/ model splitting* setting, and compare VIMADMM-J with FDML (Hu et al., 2019b) under *w/o model splitting* setting. For fair comparisons, we use the same local models for all methods and use a linear model as the server’s model. We use proposed DP mechanisms for all methods to calculate the (ϵ, δ) -DP. All experiments are run 3 times.

5.1 EVALUATION OF VANILLA VFL AND DIFFERENTIALLY PRIVATE VFL

Vanilla VFL. We observe from Figure 2 row 1 and Figure 3 row 1 that three VIM algorithms consistently outperform baselines under vanilla VFL. Specifically, (1) VIMADMM and VIMSGD converge significantly faster than VAFL on four datasets and achieve higher accuracy than VAFL especially on CIFAR, which shows that the aggregation in VIM is better than embedding averaging as in VAFL by learning separate linear weights for each client. (2) ADMM-based methods converge faster than gradient-based methods. For example, on CIFAR, VIMADMM and VIMADMM-J achieves

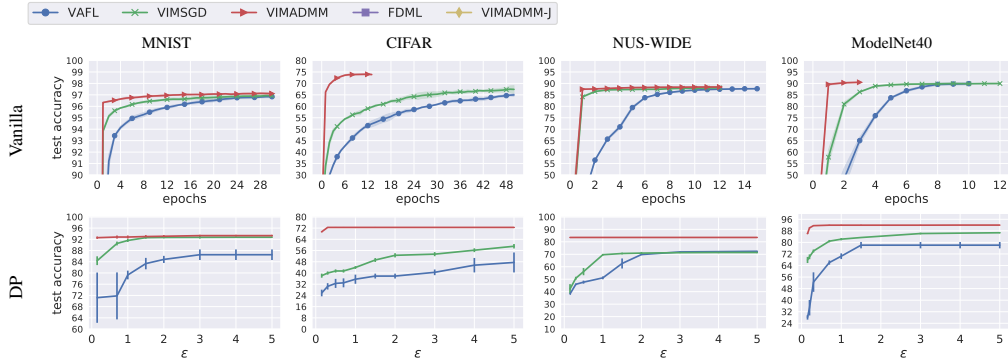


Figure 2: Performance on Vanilla and DP VFL under w/ model splitting setting. Ours outperforms baselines.

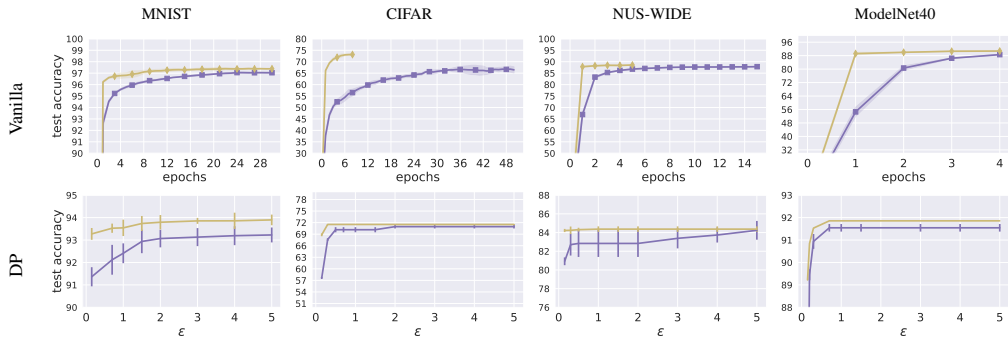


Figure 3: Performance on Vanilla and DP VFL under w/o model splitting setting. Ours outperforms baselines.

73.85%, 73.12% at epoch 8, while VAFL, VIMSGD, FDML, only achieves 46.16%, 56.26%, 56.50% at epoch 50. This is because the multiple local updates enabled by ADMM lead to better local models at each round, thereby speeding up the convergence and reducing the communication costs. For instance, each epoch consists of 44 communication rounds on CIFAR. Our VIMADMM takes 42 fewer epochs than VAFL to converge, which *saves more than 1.8k communication rounds in practice*.

Differentially Private VFL. From row 2 of Figure 2 and Figure 3, we observe that (1) three VIM algorithms always achieve higher utility than the baselines. (2) VIMADMM and VIMADMM-J reach significantly higher utility under *small* ϵ than baselines. We attribute this to the fact that the ADMM-based method converges in fewer rounds than gradient-based methods (by allowing multiple local updates at each round), which is critical to differentially private VFL since the privacy budget ϵ is consumed quickly as communication rounds increase. Therefore, our ADMM-based methods maintain higher utility.

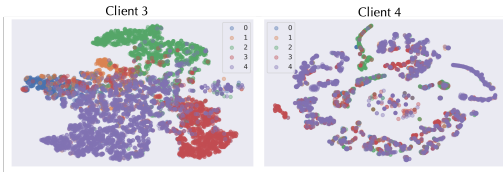


Figure 4: T-SNE of embeddings on NUS-WIDE.

Client ratio	Type	Dataset		
		MNIST	CIFAR	NUS-WIDE
100%	all	97.12 \pm 0.01	74.12 \pm 0.40	88.46 \pm 0.10
50%	important	96.58 \pm 0.07	70.28 \pm 0.44	87.29 \pm 0.17
	unimportant	78.11 \pm 0.30	62.67 \pm 2.67	75.80 \pm 0.38
20%	important	88.72 \pm 0.04	66.06 \pm 0.47	80.28 \pm 0.08
	unimportant	29.11 \pm 0.07	54.99 \pm 0.05	59.34 \pm 0.09

Table 1: Client summarization of VIMADMM.

5.2 CLIENT-LEVEL EXPLAINABILITY OF VIM

We first visualize the local embedding to justify the design of VIM, then we show that the weights of learned linear heads reflect the importance of local clients based on the weights norm histogram, which enables functionalities such as test-time noise validation, client denoising, and client summarization.

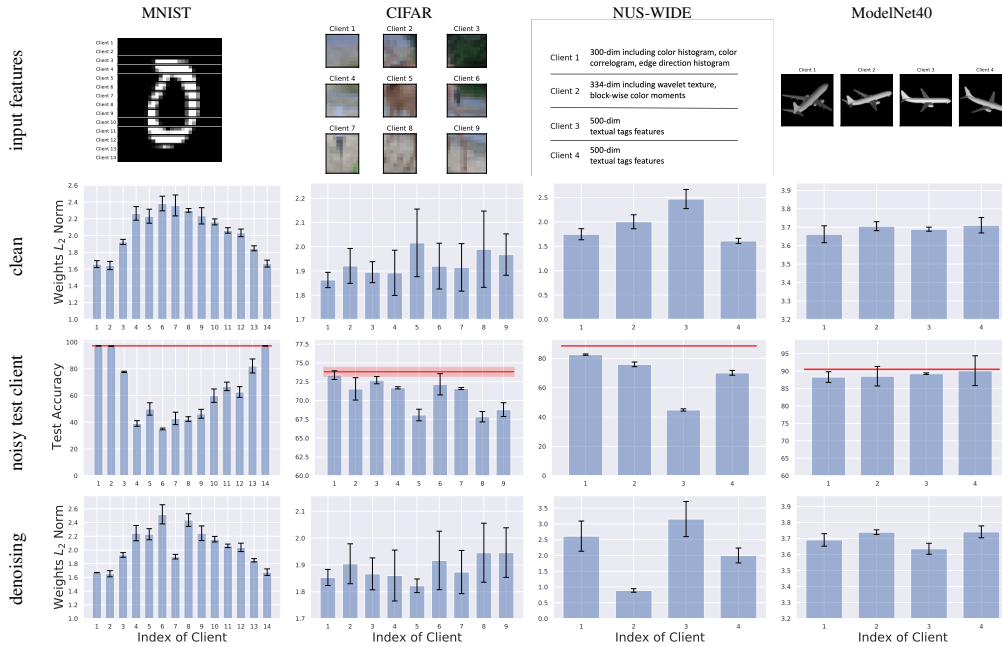


Figure 5: Row 1: input features for each client on different datasets. Row 2: histogram of the weights norm of linear head. Row 3: test accuracy when each client’s test input features are perturbed (red line denotes the test accuracy under clean test data). Row 4: histogram of the weights norm of linear head under one noisy client.

T-SNE of Local Embeddings. From the T-SNE (van der Maaten & Hinton, 2008) visualizations in Figure 4, we show that client 3 produces linear separable local embeddings (left), which are better than client 4’s embeddings (right) that overlap different classes. Therefore, the embedding averaging from VAFL (Chen et al., 2020) is suboptimal, which justifies the design of VIM, taking the properties of different local embeddings into account.

Client Importance. Given a trained VIMADMM model, we plot the weights norm of each client’s corresponding linear heads in Figure 5 row 2. Combining it with row 1, we find that *the client with important local features indeed results in high weights*¹. For example, clients 6,7,8 in MNIST holding middle rows of images that contain the center of digits, have high weights, while clients 1, 14 holding the black background pixels have low weights. A similar phenomenon is observed on CIFAR for client 5 (center) and client 1 (corner). On CIFAR, clients 8,9 also have high weights, which is because the objects on CIFAR also appear on the right bottom corner. On ModelNet40, clients have complementary views of the same objects, so their features have similar importance, leading to similar weights norms. Based on our observation, we conclude that *the weights of linear heads can reflect the importance of local clients*. We use this principle to infer that, for NUS-WIDE, the first 500 dim. of textual features have higher importance than other multimodality features, resulting in the high weights norm of client 3.

Client Importance Validation via Noisy Test Client. Given a trained VIMADMM model, we add Gaussian noise to the test local features to verify the client-level importance indicated by the linear heads. For each time, we only perturb the features of one client and keep other clients’ features unchanged. The results in Figure 5 row 3 show that *perturbing the client with high weights affects more for the test accuracy*, which verifies that clients with higher weights are more important.

Client Denoising. We study the denoising ability of VIM under training-time noisy clients. We construct one noisy client (i.e., client 7, 5, 2, 3 for MNIST, CIFAR, NUS-WIDE, ModelNet40 respectively) by adding Gaussian noise to its local features and re-train the VIMADMM model. The obtained weights norm in Figure 5 row 4 shows that VIMADMM can *automatically detect the noisy*

¹Here the weights of client refers to the weights of client’s corresponding linear head owned by the server.

client and lower its weights (compared to the clean one in Figure 5 row 2). Table 4 in Appendix B shows that under the noisy training scenario, VIMADMM and VIMSGD outperform VAFL with faster convergence and higher test accuracy.

Client Summarization. We study the functionality of client summarization enabled by VIM. (1) We first rank the importance of clients according to the weights norm histogram (i.e., Figure 5 row 2), then we select $u\%$ proportion of the most “important” clients to re-train the VIMADMM model. We find that *its performance is closed to the one trained by all clients*. Table 1 shows that the test accuracy-drop of training with 50% of the most important clients is less than 1% on MNIST and NUS-WIDE, and less than 4% on CIFAR; the accuracy-drop of training with 20% of the most important clients is less than 10% on all datasets. (2) We select $u\%$ proportion of the least important clients to re-train the model, and we find that its performance is significantly lower than the one trained with important clients, which indicates the effectiveness of VIM for client selection. (3) For the multi-view dataset ModelNet40, we find that the test accuracy of models trained with 12, 8, and 4 clients are similar, i.e., 91.04%, 90.69%, and 90.64%, suggesting that a few views can already provide sufficient training information and the agents with multiview data are of similar importance which is also reflected by our linear head weights.

6 CONCLUSIONS

In this work, we propose an efficient VFL framework with multiple linear heads (VIM). To solve our optimization problem, we propose an ADMM-based method for efficient communication. We also provide differential privacy mechanism for VIM and prove the privacy guarantee. Extensive experiments verify the superior performance of our algorithms under vanilla VFL and differentially private VFL, and show that VIM enables client-level explainability.

REFERENCES

- Opacus – train pytorch models with differential privacy, 2021. URL <https://opacus.ai/>.
- Martin Abadi, Andy Chu, Ian Goodfellow, H Brendan McMahan, Ilya Mironov, Kunal Talwar, and Li Zhang. Deep learning with differential privacy. In *Proceedings of the 2016 ACM SIGSAC conference on computer and communications security*, pp. 308–318, 2016.
- Borja Balle, Gilles Barthe, Marco Gaboardi, Justin Hsu, and Tetsuya Sato. Hypothesis testing interpretations and renyi differential privacy. In *International Conference on Artificial Intelligence and Statistics*, pp. 2496–2506. PMLR, 2020.
- Stephen Boyd, Neal Parikh, and Eric Chu. *Distributed optimization and statistical learning via the alternating direction method of multipliers*. Now Publishers Inc, 2011.
- Theodora S Brisimi, Ruidi Chen, Theofanie Mela, Alex Olshevsky, Ioannis Ch Paschalidis, and Wei Shi. Federated learning of predictive models from federated electronic health records. *International journal of medical informatics*, 112:59–67, 2018.
- Tianyi Chen, Xiao Jin, Yuejiao Sun, and Wotao Yin. Vaf1: a method of vertical asynchronous federated learning. *arXiv preprint arXiv:2007.06081*, 2020.
- Kewei Cheng, Tao Fan, Yilun Jin, Yang Liu, Tianjian Chen, Dimitrios Papadopoulos, and Qiang Yang. Secureboost: A lossless federated learning framework. *IEEE Intelligent Systems*, 36(6): 87–98, 2021.
- Tat-Seng Chua, Jinhui Tang, Richang Hong, Haojie Li, Zhiping Luo, and Yantao Zheng. Nus-wide: a real-world web image database from national university of singapore. In *Proceedings of the ACM international conference on image and video retrieval*, pp. 1–9, 2009.
- Jinshuo Dong, Aaron Roth, and Weijie J Su. Gaussian differential privacy. *arXiv preprint arXiv:1905.02383*, 2019.
- Cynthia Dwork. A firm foundation for private data analysis. *Communications of the ACM*, 54(1): 86–95, 2011.

-
- Cynthia Dwork and Aaron Roth. The algorithmic foundations of differential privacy. *Foundations and Trends in Theoretical Computer Science*, 9(3-4):211–407, 2014.
- Cynthia Dwork, Krishnaram Kenthapadi, Frank McSherry, Ilya Mironov, and Moni Naor. Our data, ourselves: Privacy via distributed noise generation. In *Advances in Cryptology – EUROCRYPT*, 2006.
- Anis Elgabli, Jihong Park, Sabbir Ahmed, and Mehdi Bennis. L-fgadm: Layer-wise federated group adm for communication efficient decentralized deep learning. In *2020 IEEE Wireless Communications and Networking Conference (WCNC)*, pp. 1–6. IEEE, 2020a.
- Anis Elgabli, Jihong Park, Amrit S Bedi, Mehdi Bennis, and Vaneet Aggarwal. Gadm: Fast and communication efficient framework for distributed machine learning. *J. Mach. Learn. Res.*, 21(76): 1–39, 2020b.
- Siwei Feng and Han Yu. Multi-participant multi-class vertical federated learning. *arXiv preprint arXiv:2001.11154*, 2020.
- Chong Fu, Xuhong Zhang, Shouling Ji, Jinyin Chen, Jingzheng Wu, Shanqing Guo, Jun Zhou, Alex X Liu, and Ting Wang. Label inference attacks against vertical federated learning. In *31st USENIX Security Symposium (USENIX Security 22)*, Boston, MA, August 2022. USENIX Association. URL <https://www.usenix.org/conference/usenixsecurity22/presentation/fu>.
- Bin Gu, Zhiyuan Dang, Xiang Li, and Heng Huang. Federated doubly stochastic kernel learning for vertically partitioned data. In *Proceedings of the 26th ACM SIGKDD International Conference on Knowledge Discovery & Data Mining*, pp. 2483–2493, 2020.
- Andrew Hard, Kanishka Rao, Rajiv Mathews, Françoise Beaufays, Sean Augenstein, Hubert Eichner, Chloé Kiddon, and Daniel Ramage. Federated learning for mobile keyboard prediction. *arXiv preprint arXiv:1811.03604*, 2018.
- Stephen Hardy, Wilko Henecka, Hamish Ivey-Law, Richard Nock, Giorgio Patrini, Guillaume Smith, and Brian Thorne. Private federated learning on vertically partitioned data via entity resolution and additively homomorphic encryption. *arXiv preprint arXiv:1711.10677*, 2017.
- Kaiming He, Xiangyu Zhang, Shaoqing Ren, and Jian Sun. Deep residual learning for image recognition. In *Proceedings of the IEEE conference on computer vision and pattern recognition*, pp. 770–778, 2016.
- Yaochen Hu, Peng Liu, Linglong Kong, and Di Niu. Learning privately over distributed features: An adm sharing approach. *arXiv preprint arXiv:1907.07735*, 2019a.
- Yaochen Hu, Di Niu, Jianming Yang, and Shengping Zhou. Fdml: A collaborative machine learning framework for distributed features. In *Proceedings of the 25th ACM SIGKDD International Conference on Knowledge Discovery & Data Mining*, pp. 2232–2240, 2019b.
- Zonghao Huang, Rui Hu, Yuanxiong Guo, Eric Chan-Tin, and Yanmin Gong. Dp-admm: Admm-based distributed learning with differential privacy. *IEEE Transactions on Information Forensics and Security*, 15:1002–1012, 2019.
- Xiao Jin, Pin-Yu Chen, Chia-Yi Hsu, Chia-Mu Yu, and Tianyi Chen. Catastrophic data leakage in vertical federated learning. *Advances in Neural Information Processing Systems*, 34, 2021.
- Yan Kang, Yang Liu, and Tianjian Chen. Fedmvt: Semi-supervised vertical federated learning with multiview training. *arXiv preprint arXiv:2008.10838*, 2020.
- Prannay Khosla, Piotr Teterwak, Chen Wang, Aaron Sarna, Yonglong Tian, Phillip Isola, Aaron Maschiot, Ce Liu, and Dilip Krishnan. Supervised contrastive learning. *Advances in Neural Information Processing Systems*, 33:18661–18673, 2020.
- Alex Krizhevsky. Learning multiple layers of features from tiny images. Technical report, 2009.

-
- Yann LeCun and Corinna Cortes. MNIST handwritten digit database. 2010. URL <http://yann.lecun.com/exdb/mnist/>.
- Yang Liu, Yan Kang, Xinwei Zhang, Liping Li, Yong Cheng, Tianjian Chen, Mingyi Hong, and Qiang Yang. A communication efficient collaborative learning framework for distributed features. *arXiv preprint arXiv:1912.11187*, 2019.
- Brendan McMahan, Eider Moore, Daniel Ramage, Seth Hampson, and Blaise Aguera y Arcas. Communication-Efficient Learning of Deep Networks from Decentralized Data. In *Proceedings of the 20th International Conference on Artificial Intelligence and Statistics*, volume 54 of *Proceedings of Machine Learning Research*, pp. 1273–1282. PMLR, 20–22 Apr 2017.
- Ilya Mironov. Rényi differential privacy. In *2017 IEEE 30th computer security foundations symposium (CSF)*, pp. 263–275. IEEE, 2017.
- Nicolas Papernot, Patrick McDaniel, Arunesh Sinha, and Michael P Wellman. Sok: Security and privacy in machine learning. In *2018 IEEE European Symposium on Security and Privacy (EuroS&P)*, pp. 399–414. IEEE, 2018.
- Adam Paszke, Sam Gross, Francisco Massa, Adam Lerer, James Bradbury, Gregory Chanan, Trevor Killeen, Zeming Lin, Natalia Gimelshein, Luca Antiga, Alban Desmaison, Andreas Kopf, Edward Yang, Zachary DeVito, Martin Raison, Alykhan Tejani, Sasank Chilamkurthy, Benoit Steiner, Lu Fang, Junjie Bai, and Soumith Chintala. Pytorch: An imperative style, high-performance deep learning library. In H. Wallach, H. Larochelle, A. Beygelzimer, F. d'Alché-Buc, E. Fox, and R. Garnett (eds.), *Advances in Neural Information Processing Systems 32*, pp. 8024–8035. Curran Associates, Inc., 2019. URL <http://papers.neurips.cc/paper/9015-pytorch-an-imperative-style-high-performance-deep-learning-library.pdf>.
- Alec Radford, Jong Wook Kim, Chris Hallacy, Aditya Ramesh, Gabriel Goh, Sandhini Agarwal, Girish Sastry, Amanda Askell, Pamela Mishkin, Jack Clark, et al. Learning transferable visual models from natural language supervision. In *International Conference on Machine Learning*, pp. 8748–8763. PMLR, 2021.
- Jong-Chyi Su, Matheus Gadelha, Rui Wang, and Subhransu Maji. A deeper look at 3d shape classifiers. In *Second Workshop on 3D Reconstruction Meets Semantics, ECCV*, 2018.
- Laurens van der Maaten and Geoffrey Hinton. Visualizing data using t-sne. *Journal of Machine Learning Research*, 9(86):2579–2605, 2008. URL <http://jmlr.org/papers/v9/vandermaaten08a.html>.
- Praneeth Vepakomma, Otkrist Gupta, Tristan Swedish, and Ramesh Raskar. Split learning for health: Distributed deep learning without sharing raw patient data. *arXiv preprint arXiv:1812.00564*, 2018.
- Yu-Xiang Wang, Borja Balle, and Shiva Prasad Kasiviswanathan. Subsampled rényi differential privacy and analytical moments accountant. In *The 22nd International Conference on Artificial Intelligence and Statistics*, pp. 1226–1235. PMLR, 2019.
- Yuncheng Wu, Shaofeng Cai, Xiaokui Xiao, Gang Chen, and Beng Chin Ooi. Privacy preserving vertical federated learning for tree-based models. *Proceedings of the VLDB Endowment*, 13(12): 2090–2103, 2020.
- Qiang Yang, Yang Liu, Tianjian Chen, and Yongxin Tong. Federated machine learning: Concept and applications. *ACM Transactions on Intelligent Systems and Technology (TIST)*, 10(2):12, 2019a.
- Shengwen Yang, Bing Ren, Xuhui Zhou, and Liping Liu. Parallel distributed logistic regression for vertical federated learning without third-party coordinator. *arXiv preprint arXiv:1911.09824*, 2019b.
- Timothy Yang, Galen Andrew, Hubert Eichner, Haicheng Sun, Wei Li, Nicholas Kong, Daniel Ramage, and Françoise Beaufays. Applied federated learning: Improving google keyboard query suggestions. *arXiv preprint arXiv:1812.02903*, 2018.

-
- Wensi Yang, Yuhang Zhang, Kejiang Ye, Li Li, and Cheng-Zhong Xu. Ffd: a federated learning based method for credit card fraud detection. In *International Conference on Big Data*, pp. 18–32. Springer, 2019c.
- Sheng Yue, Ju Ren, Jiang Xin, Sen Lin, and Junshan Zhang. Inexact-admm based federated meta-learning for fast and continual edge learning. In *Proceedings of the Twenty-second International Symposium on Theory, Algorithmic Foundations, and Protocol Design for Mobile Networks and Mobile Computing*, pp. 91–100, 2021.
- Qingsong Zhang, Bin Gu, Cheng Deng, and Heng Huang. Secure bilevel asynchronous vertical federated learning with backward updating. In *Proceedings of the AAAI Conference on Artificial Intelligence*, volume 35, pp. 10896–10904, 2021.
- Ciyou Zhu, Richard H Byrd, Peihuang Lu, and Jorge Nocedal. Algorithm 778: L-bfgs-b: Fortran subroutines for large-scale bound-constrained optimization. *ACM Transactions on mathematical software (TOMS)*, 23(4):550–560, 1997.

A ALGORITHM DETAILS

A.1 VIMSGD

At each communication round t , the server samples a set of data indices, $B(t)$, with batch size $|B(t)| = b$. Then we describe the key steps of VIMSGD as follows:

(1) Communication from client to server. Each client k sends a batch of embeddings $\{h_j^{k(t)}\}_{j \in B(t)}$ to the server, where $h_j^{k(t)} = f(x_j^k, \theta_k^{(t)})$, $\forall j \in B(t)$.

(2) Server updates linear heads $\{W_k\}$. According to VIM objective in Eq. 2, each linear head of the server is updated as:

$$W_k^{(t+1)} \leftarrow W_k^{(t)} - \eta \nabla_{W_k^{(t)}} \mathcal{L}_{\text{VIM}}(W_k^{(t)}), \forall k \in [M] \quad (12)$$

where η is the server learning rate, and

$$\nabla_{W_k^{(t)}} \mathcal{L}_{\text{VIM}}(W_k^{(t)}) = \nabla_{W_k^{(t)}} \left(\sum_{j=1}^N \ell \left(\sum_{i=1}^M h_j^{i(t)} W_i^{(t)}; y_j \right) + \beta \mathcal{R}(W_k^{(t)}) \right) \quad (13)$$

(3) Communication from server to client. Server computes gradients w.r.t each local embedding $\nabla_{h_j^{k(t)}} \mathcal{L}_{\text{VIM}}(W_k^{(t+1)})$ by the VIM objective in Eq. 2, where

$$\nabla_{h_j^{k(t)}} \mathcal{L}_{\text{VIM}}(W_k^{(t+1)}) = \nabla_{h_j^{k(t)}} \ell \left(\sum_{i=1}^M h_j^{i(t)} W_i^{(t+1)}; y_j \right), \forall j \in B(t), k \in [M] \quad (14)$$

Server sends gradients $\{\nabla_{h_j^{k(t)}} \mathcal{L}_{\text{VIM}}(W_k^{(t+1)})\}_{j \in B(t)}$ to each client k , $\forall k \in [M]$.

(4) Client updates local model parameters θ_k . Finally, every client k locally updates the model parameters θ_k according to the VIM objective in Eq. 2 as follows:

$$\theta_k^{(t+1)} = \theta_k^{(t)} - \eta^k \nabla_{\theta_k^{(t)}} \mathcal{L}_{\text{VIM}}(W_k^{(t+1)}), \forall k \in [M] \quad (15)$$

where η^k is the local learning rate for client k , and

$$\nabla_{\theta_k^{(t)}} \mathcal{L}_{\text{VIM}}(W_k^{(t+1)}) = \sum_{j=1}^N \nabla_{\theta_k^{(t)}} h_j^{k(t)} \nabla_{h_j^{k(t)}} \mathcal{L}_{\text{VIM}}(W_k^{(t+1)}) + \beta \nabla_{\theta_k^{(t)}} \mathcal{R}(\theta_k^{(t)}) \quad (16)$$

These four steps of VIMSGD are summarized in Algorithm 2.

A.2 VIMADMM-J

At each communication round t , the server samples a set of data indices, $B(t)$, with batch size $|B(t)| = b$. Then we describe the key steps of VIMADMM-J as follows:

(1) Communication from client to server. Each client k sends a batch of local logits $\{o_j^{k(t)}\}_{j \in B(t)}$ to the server, where $o_j^{k(t)} = f(x_j^k, \theta_k^{(t)}) W_k^{(t)}$, $\forall j \in B(t)$

(2) Server updates auxiliary variables $\{z_j\}$. After receiving the local logits from all clients, the server updates the auxiliary variable for each sample j as:

$$z_j^{(t+1)} = \underset{z_j}{\operatorname{argmin}} \quad \ell(z_j; y_j) - \lambda_j^{(t)\top} z_j + \frac{\rho}{2} \left\| \sum_{k=1}^M o_j^{k(t)} - z_j \right\|_F^2, \forall j \in B(t) \quad (17)$$

Since the optimization problem in Eq. 17 is convex and differentiable with respect to z_j , we use the L-BFGS-B algorithm (Zhu et al., 1997) to solve the minimization problem.

Algorithm 2: VIMSGD (Changes for differential privacy highlighted in gray)

Input: number of communication rounds T , number of clients M , number of training samples N , batch size b , input features $\{\{x_j^1\}_{j=1}^N, \{x_j^2\}_{j=1}^N, \dots, \{x_j^M\}_{j=1}^N\}$, the labels $\{y_j\}_{j=1}^N$, local model $\{\theta_k\}_{k=1}^M$; linear heads $\{W_k\}_{k=1}^M$; server learning rate η ; client learning rate $\{\eta^k\}_{k=1}^M$; noise parameter σ , clipping constant C

1 **for** communication round $t \in [T]$ **do**
2 Server samples a set of data indices $B(t)$ with $|B(t)| = b$
3 **for** client $k \in [M]$ **do**
4 **generates** a local training batch $\{x_j^k\}_{j \in B(t)}$
5 **computes** local embeddings $h_j^{k(t)} \leftarrow f(x_j^k, \theta_k), \forall j \in B(t)$
6 **clips and perturbs** local embeddings $h_j^{k(t)} \leftarrow \text{Clip}(h_j^{k(t)}, C) + \mathcal{N}(0, \sigma^2 C^2), \forall j \in B(t)$
7 **sends** local embeddings $\{h_j^{k(t)}\}_{j \in B(t)}$ to the server
8 Server **updates** linear heads $W_k^{(t+1)}$ by Eq. 12, $\forall k \in [M]$
9 Server **computes** gradients w.r.t embeddings $\nabla_{h_j^{k(t)}} \mathcal{L}_{\text{VIM}}(W_k^{(t+1)})$ by Eq. 14, $\forall j \in B(t), k \in [M]$
10 Server **sends** gradients $\{\nabla_{h_j^{k(t)}} \mathcal{L}_{\text{VIM}}(W_k^{(t+1)})\}_{j \in B(t)}$ to each client $k, \forall k \in [M]$
11 **for** client $k \in [M]$ **do**
12 **updates** local model $\theta_k^{(t+1)}$ by Eq. 15

(3) *Server updates dual variables* $\{\lambda_j\}$. After the updates in Eq. 17, the server updates the dual variable for each sample j as:

$$\lambda_j^{(t+1)} = \lambda_j^{(t)} + \rho \left(\sum_{k=1}^M o_j^{k(t)} - z_j^{(t+1)} \right), \forall j \in B(t) \quad (18)$$

(4) *Communication from server to client.* After the updates in Eq. 18, we define a residual variable $s_j^{k(t+1)}$ for each sample j of k -th client, which provides supervision for updating local model:

$$s_j^{k(t+1)} \triangleq z_j^{(t+1)} - \sum_{i \in [M], i \neq k} o_j^{i(t)} \quad (19)$$

The server sends the dual variables $\{\lambda_j^{(t+1)}\}_{j \in B(t)}$ and the residual variables $\{s_j^{k(t+1)}\}_{j \in B(t)}$ of all samples to each client k .

(5) *Client updates linear head W_k and local model θ_k alternatively.* The linear head of each client is locally updated as:

$$W_k^{(t+1)} = \underset{W_k}{\operatorname{argmin}} \quad \beta \mathcal{R}(W_k) + \sum_{j \in B(t)} \lambda_j^{(t+1)\top} f(x_{j_k}, \theta_k^{(t)}) W_k + \sum_{j \in B(t)} \frac{\rho}{2} \left\| s_j^{k(t+1)} - f(x_{j_k}, \theta_k^{(t)}) W_k \right\|_F^2, \forall k \in [M]. \quad (20)$$

Each client updates the local model parameters θ_k as follows:

$$\theta_k^{(t+1)} = \underset{\theta_k}{\operatorname{argmin}} \quad \beta \mathcal{R}(\theta_k) + \sum_{j \in B(t)} \lambda_j^{(t+1)\top} f(x_{j_k}, \theta_k) W_k^{(t+1)} + \sum_{j \in B(t)} \frac{\rho}{2} \left\| s_j^{k(t+1)} - f(x_{j_k}, \theta_k) W_k^{(t+1)} \right\|_F^2. \quad (21)$$

Due to the nonconvexity of the loss function of DNN, we use τ local steps of SGD to update W_k and θ_k alternatively at each round with the objective of Eq. 20 and Eq. 21. Specifically, at each local step, we first update W_k and then update θ_k .

These five steps of VIMADMM are summarized in Algorithm 3.

Algorithm 3: VIMADMM-J (Differentially Private VIMADMM-J)

Input: number of communication rounds T , number of clients M , number of training samples N , batch size b , input features $\{\{x_j^1\}_{j=1}^N, \{x_j^2\}_{j=1}^N, \dots, \{x_j^M\}_{j=1}^N\}$, the labels $\{y_j\}_{j=1}^N$, local model $\{\theta_k\}_{k=1}^M$; linear heads $\{W_k\}_{k=1}^M$; auxiliary variables $\{z_j\}_{j=1}^N$; dual variables $\{\lambda_j\}_{j=1}^N$; noise parameter σ , clipping constant C

```
1 for communication round  $t \in [T]$  do
2   Server samples a set of data indices  $B(t)$  with  $|B(t)| = b_s$ 
3   for client  $k \in [M]$  do
4     generates a local training batch  $\{x_j^k\}_{j \in B(t)}$ 
5     computes local logits  $o_j^{k(t)} = f(x_j^k, \theta_k^{(t)})W_k^{(t)}, \forall j \in B(t)$ 
6     clips and perturbs local logits  $o_j^{k(t)} \leftarrow o_j^{k(t)} / \max\left(1, \left\|o_j^{k(t)}\right\|_2 / C\right) + \mathcal{N}(0, \sigma^2 C^2), \forall j \in B(t)$ 
7     sends local logits  $\{o_j^{k(t)}\}_{j \in B(t)}$  to the server
8   Server updates auxiliary variables  $z_j^{(t+1)}$  via Eq. 17,  $\forall j \in B(t)$ 
9   Server updates dual variables  $\lambda_j^{(t+1)}$  via Eq. 18,  $\forall j \in B(t)$ 
10  Server computes residual variables  $s_j^{k(t+1)}$  via Eq. 19,  $\forall j \in B(t), k \in [M]$ 
11  Server sends  $\{\lambda_j^{(t+1)}\}_{j \in B(t)}, \{s_j^{k(t+1)}\}_{j \in B(t)}$  to each client  $k, \forall k \in [M]$ 
12  for client  $k \in [M]$  do
13    for local step  $e \in [\tau]$  do
14      updates local linear head  $W_k^{(t+1)}$  via SGD with objective of Eq. 20
15      updates local model  $\theta_k^{(t+1)}$  via SGD with objective of Eq. 21
```

B EXPERIMENTAL DETAILS

B.1 DATASETS AND MODELS

We consider a diverse set of datasets and tasks.

- MNIST (LeCun & Cortes, 2010) contains images with handwritten digits. We create the VFL scenario by splitting the input features evenly by rows for 14 clients. We use a fully connected model of two linear layers with ReLU activations as the local model.
- CIFAR (Krizhevsky, 2009) contains colour images. We split each image into patches for 9 clients. We use a standard CNN architecture from the PyTorch library (opa, 2021) as the local model.
- NUS-WIDE (Chua et al., 2009) is a multi-modality dataset with 634 low-level image features and 1000 textual tag features. We distribute image features to 2 clients (300 dim and 334 dim), and text features to 2 clients (500 dim and 500 dim). We use a fully connected model of two linear layers with ReLU activations as the local model.
- ModelNet40 (Su et al., 2018) is a multi-view image dataset, containing the shaded images from 12 views for the same objects. We use 4 views and distribute them to 4 clients respectively. We use ResNet-18 (He et al., 2016) as the local model.

We split each dataset into the train, validation, and test sets. See Table 2 for more details about the number of samples and the number of classes for each dataset.

B.2 PLATFORM

We simulate the vertical federated learning setup (1 server and N users) on a Linux machine with AMD Ryzen Threadripper 3990X 64-Core CPUs and 4 NVIDIA GeForce RTX 3090 GPUs. The algorithms are implemented by PyTorch (Paszke et al., 2019). Please see the submitted code for full details. We run each experiment 3 times with different random seeds.

B.3 HYPERPARAMETERS

We detail our hyperparameter tuning protocol and the hyperparameter values here. For all VFL training experiments, we use the SGD optimizer with learning rate η for the server’s model, and the SGD optimizer with momentum 0.9 and learning rate η^k for client k ’s local model. We set $\eta = \eta^1, \eta^2, \dots, \eta^M$ for all methods. The regularization weight β is set to 0.005. The embedding dimension d_f is set to 60, and batch size b is set to 1024 for all datasets.

Vanilla VFL Training For Vanilla VFL training experiments, we tune learning rates by performing a grid search separately for all methods over $\{0.1, 0.3, 0.5, 0.8\}$ on MNIST, $\{0.003, 0.005, 0.008, 0.01, 0.05, 0.1\}$ on CIFAR, $\{0.1, 0.5\}$ on NUS-WIDE, $\{0.0005, 0.005, 0.01, 0.05, 0.1\}$ on ModelNet40. Table 2 summarize hyperparameters for all methods.

Table 2: Dataset description and hyperparameters for Vanilla VFL Training.

Dataset	# features	d_c	N	# samples			VAFL	VIMSGD	VIMADMM	FDML	VIMADMM-J					
				train	validation	test	η	η	η	ρ	τ	η	η	ρ	τ	
MNIST	28×28	10	14	54000	6000	10000	0.3	0.3	0.05	2	20	0.1	0.05	0.5	20	
CIFAR	$32 \times 32 \times 3$	10	9	45000	5000	10000	0.003	0.005	0.005	2	30	0.005	0.005	0.05	2	30
NUS-WIDE	1634	5	4	54000	6000	10000	0.1	0.5	0.05	2	20	0.1	0.05	2	20	
ModelNet40	$224 \times 224 \times 3 \times N$	40	4	8877	966	2468	0.05	0.05	0.05	0.5	5	0.05	0.05	0.5	5	

Differentially Private VFL Training We leverage the PyTorch Differential Privacy library Opacus (opa, 2021) version 0.15.0 to calculate the privacy budgets ϵ . In all experiments, $\delta = 1e - 5$. For each privacy budget ϵ , we perform a grid search for the combination of hyperparameters (including noise scale σ , clipping threshold C , and learning rate η) for all methods for a fair comparison. The noise scale is tuned from $\sigma \{2, 3, 5, 8, 10, 20\}$ on all datasets. C is tuned from $\{0.01, 0.05, 0.1, 0.3\}$ and η is tuned from $\{0.05, 0.3, 0.5, 1\}$ for MNIST; C is tuned from $\{0.01, 0.05, 0.1, 0.5, 1\}$ and η is tuned from $\{0.005, 0.01, 0.05, 0.1\}$ for CIFAR; C is tuned from $\{0.01, 0.05, 0.1, 0.3\}$ and η is tuned from $\{0.05, 0.1, 0.3, 0.5, 1\}$ for NUS-WIDE; C is tuned from $\{0.1, 0.5, 1\}$ and η is tuned from $\{0.05, 0.1, 0.5\}$ for ModelNet40. We list the optimal hyper-parameter values (noise scale σ , clipping threshold C , and learning rate η) for private VFL training under privacy budget $\epsilon = 1$ in Table 3 for four datasets. We use the best hyper-parameters to start 3 runs with different random seeds and report the average results for each method.

Table 3: Optimal hyper-parameter values (noise scale σ , clipping threshold C , and learning rate η) for different methods with privacy budget $\epsilon = 1$.

Dataset	VAFL	VIMSGD	VIMADMM	FDML	VIMADMM-J
MNIST	(2, 0.3, 0.5)	(2, 0.3, 0.5)	(10, 0.01, 0.05)	(2, 0.1, 0.5)	(5, 0.05, 0.05)
CIFAR	(2, 0.5, 0.05)	(2, 0.5, 0.01)	(20, 0.01, 0.005)	(20, 0.5, 0.005)	(20, 0.01, 0.005)
NUS-WIDE	(2, 0.3, 0.1)	(2, 0.3, 0.3)	(10, 0.01, 0.05)	(20, 0.05, 0.1)	(2, 0.1, 0.05)
ModelNet40	(10, 0.1, 0.1)	(10, 0.1, 0.1)	(10, 0.1, 0.05)	(20, 1, 0.05)	(10, 0.1, 0.05)

Client-level Explainability In the experiments of *client importance validation via noisy test client*, for each time, we perturb the features of all test samples at one client by adding Gaussian noise sampled from $\mathcal{N}(0, \bar{\sigma}^2)$ to its features. In order to observe the difference in test accuracy between important clients and unimportant clients, we set $\bar{\sigma}$ to 10 for MNIST, 1 for CIFAR and NUS-WIDE, and 3 for ModelNet40.

In the experiments of *client denoising*, we construct one noisy client (i.e., client 7, 5, 2, 3 for MNIST, CIFAR, NUS-WIDE, ModelNet40 respectively) by adding Gaussian noise sampled from $\mathcal{N}(0, \tilde{\sigma}^2)$ to all its training samples and test samples. We set $\tilde{\sigma}$ to 1 for MNIST, NUS-WIDE and ModelNet40, and 3 for CIFAR.

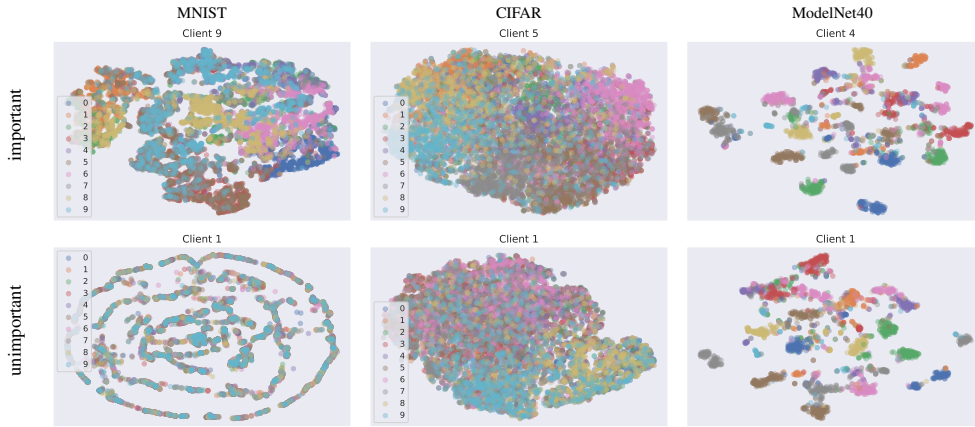


Figure 6: T-SNE visualizations of local embeddings from important client and unimportant client for VIMADMM.

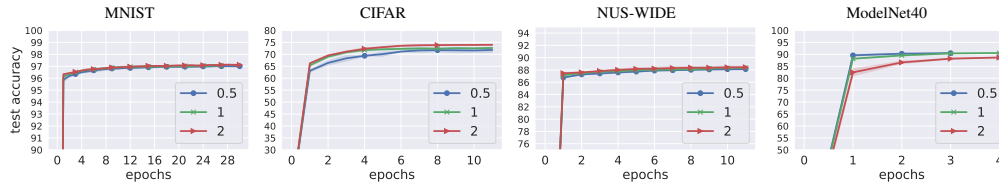


Figure 7: Test accuracy of VIMADMM with different penalty factor ρ on four datasets.

B.4 ADDITIONAL RESULTS

Additional Results on T-SNE of Local Embeddings. Figure 6 presents the T-SNE visualizations of local embeddings for the model trained from VIMADMM. Similar to the results of NUS-WIDE in Figure 4, Figure 6 shows that important clients learn better local embeddings than unimportant clients on MNIST and CIFAR, which justifies our design of multiple linear heads in VIM. For ModelNet40, since clients with multi-view data are of similar importance, their local embeddings are similar and are linearly separable.

Additional Results on Client Denoising Table 4 presents the test accuracy of VAFL, VIMSGD, and VIMADMM at different epochs (communication rounds) on different datasets under one noisy client. Note that each epoch consists of N/b communication rounds. Table 4 shows that under the noisy training scenario, VIMADMM and VIMSGD consistently outperform VAFL with faster convergence and higher test accuracy, which indicates the effectiveness of VIM’s multiple linear heads in client denoising.

Table 4: Test accuracy under one noisy client whose training local features and test local features are perturbed by Gaussian noise.

Method	Test accuracy @ epoch (communication round)											
	MNIST			CIFAR			NUS-WIDE			ModelNet40		
	2 (106)	5 (265)	10 (530)	2 (88)	5 (220)	10 (440)	2 (106)	5 (265)	10 (530)	2 (18)	5 (45)	10 (90)
VAFL	91.07 ± 0.17	94.36 ± 0.16	95.59 ± 0.11	28.83 ± 1.04	38.77 ± 0.39	46.98 ± 0.70	51.88 ± 0.72	77.68 ± 0.74	85.31 ± 0.15	43.23 ± 3.07	80.13 ± 1.10	89.56 ± 0.41
VIMSGD	95.04 ± 0.14	96.01 ± 0.03	96.43 ± 0.08	42.75 ± 0.13	50.06 ± 0.18	55.53 ± 0.37	85.35 ± 0.24	86.42 ± 0.24	87.14 ± 0.29	77.94 ± 1.00	88.74 ± 0.07	89.69 ± 0.42
VIMADMM	96.22 ± 0.07	96.60 ± 0.04	96.82 ± 0.07	67.08 ± 0.43	70.70 ± 0.34	71.76 ± 0.14	86.38 ± 0.20	87.00 ± 0.27	87.18 ± 0.14	90.05 ± 0.38	90.71 ± 0.31	90.59 ± 0.05

Effect of Penalty Factor ρ for VIMADMM Figure 7 presents the test accuracy of VIMADMM with different penalty factor ρ . The results on four datasets show that VIMADMM is not sensitive to ρ and we suggest that the practitioners choose the optimal ρ from 0.5 to 2, which will not influence the test accuracy significantly.

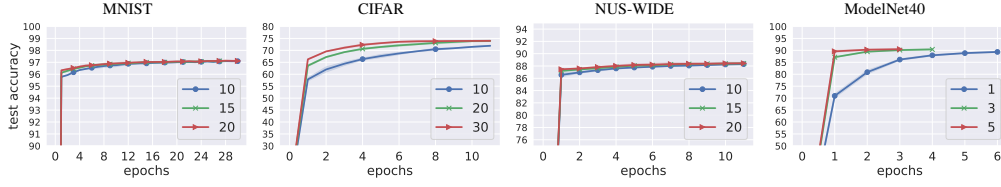


Figure 8: Test accuracy of VIMADMM with different local steps τ on four datasets.

Effect of Local Steps τ for VIMADMM Figure 7 presents the test accuracy of VIMADMM with different local steps τ . The results on four datasets show when τ is larger, the VIMADMM algorithm converges faster. This is because the local models can be trained better with more local update steps (i.e., larger τ) at each communication round. Therefore, we suggest that the practitioners choose a τ that leads to the converged local model at each communication round.

C DIFFERENTIAL PRIVATE ANALYSES

C.1 PRELIMINARIES

We utilize Rényi Differential Privacy (RDP) to perform the privacy analysis since it supports a tighter composition of privacy budget (Mironov, 2017) than the moments accounting technique (Abadi et al., 2016) for Differential Privacy (DP).

We start by introducing the definition of RDP as a generalization of DP, which leverages the α -Rényi divergence between the output distributions of two neighboring datasets. The definition of the neighboring dataset in this work follows the standard differentially private machine learning framework (Abadi et al., 2016). The neighboring datasets would differ in a single entry, that is, one data instance is present or absent in one dataset.

Definition 2. (Rényi Differential Privacy (Mironov, 2017)) We say that a mechanism \mathcal{M} is (α, ϵ) -RDP with order $\alpha \in (1, \infty)$ if for all neighboring datasets D, D'

$$D_\alpha(\mathcal{M}(D) \parallel \mathcal{M}(D')) := \frac{1}{\alpha - 1} \log \mathbb{E}_{\theta \sim \mathcal{M}(D')} \left[\left(\frac{\mathcal{M}(D)(\theta)}{\mathcal{M}(D')(\theta)} \right)^\alpha \right] \leq \epsilon \quad (22)$$

RDP guarantee can be converted to DP guarantee as follows:

Theorem 2. (RDP to (ϵ, δ) -DP Conversion (Balle et al., 2020))² If f is an (α, ϵ) -RDP mechanism, it also satisfies $(\epsilon + \log \frac{\alpha-1}{\alpha} - \frac{\log \delta + \log \alpha}{\alpha-1}, \delta)$ -differential privacy for any $0 < \alpha < 1$.

Here, we highlight three key properties that are relevant to our analyses.

Theorem 3. (RDP Composition (Mironov, 2017)) Let $f : \mathcal{D} \mapsto \mathcal{R}_1$ be (α, ϵ_1) -RDP and $g : \mathcal{R}_1 \times \mathcal{D} \mapsto \mathcal{R}_2$ be (α, ϵ_2) -RDP, then the mechanism defined as (X, Y) , where $X \sim f(D)$ and $Y \sim g(X, D)$, satisfies $(\alpha, \epsilon_1 + \epsilon_2)$ -RDP.

Theorem 4. (RDP Guarantee for Gaussian Mechanism (Mironov, 2017)) If f is a real-valued function, the Gaussian Mechanism for approximating f is defined as $\mathbf{G}_\sigma f(D) = f(D) + \mathcal{N}(0, \sigma^2)$. If f has ℓ_2 sensitivity 1, then the Gaussian Mechanism $\mathbf{G}_\sigma f$ satisfies $(\alpha, \alpha/(2\sigma^2))$ -RDP.

Theorem 5. (RDP for Subsampled Mechanisms (Wang et al., 2019)) Given a dataset of n points drawn from a domain \mathcal{X} and a (randomized) mechanism \mathcal{M} that takes an input from \mathcal{X}^m for $m \leq n$, let the randomized algorithm $\mathcal{M} \circ \text{subsample}$ be defined as: (1) subsample: subsample without replacement m datapoints of the dataset (sampling parameter $\gamma = m/n$), and (2) apply \mathcal{M} : a randomized algorithm taking the subsampled dataset as the input. For all integers $\alpha \geq 2$, if \mathcal{M} obeys $(\alpha, \epsilon(\alpha))$ -RDP, then this new randomized algorithm $\mathcal{M} \circ \text{subsample}$ obeys $(\alpha, \epsilon'(\alpha))$ -RDP

²This theorem is tighter than the original RDP paper (Mironov, 2017), and it is adopted in the official implementation of the PyTorch Opacus library (opa, 2021).

where,

$$\begin{aligned} \epsilon'(\alpha) \leq & \frac{1}{\alpha-1} \log \left(1 + \gamma^2 \binom{\alpha}{2} \min \left\{ 4 \left(e^{\epsilon(2)} - 1 \right), e^{\epsilon(2)} \min \left\{ 2, \left(e^{\epsilon(\infty)} - 1 \right)^2 \right\} \right\} \right) \\ & + \sum_{j=3}^{\alpha} \gamma^j \binom{\alpha}{j} e^{(j-1)\epsilon(j)} \min \left\{ 2, \left(e^{\epsilon(\infty)} - 1 \right)^j \right\} \end{aligned}$$

C.2 PROOF OF THEOREM 1

We aim to protect the privacy of local training dataset (i.e., feature set) $X_k = \{x_j^k\}_{j=1}^N$ of each client k . We consider the output of client k at each communication round t as a matrix, where each row is the embedding or logit of one training sample. With a loss of generality, we consider the embeddings as local output.

We first define a function \mathcal{H} that outputs the matrix of clipped embeddings for input dataset X_k :

$$\mathcal{H}(X_k) = [\hat{h}_1^k, \dots, \hat{h}_N^k], \text{ where } \hat{h}_j^k = \text{Clip}(f(x_j^k, \theta_k), C), \forall j \in [N]. \quad (23)$$

Lemma 1. *For any neighboring datasets X_k, X'_k differing by one data sample, the ℓ_2 sensitivity for \mathcal{H} is C .*

Proof. WLOG, the neighboring dataset X'_k differs the first training sample, i.e., $X'_k = \{x_1^{k'}, x_2^k, \dots, x_N^k\}$. The ℓ_2 sensitivity for \mathcal{H} is bounded as follows:

$$\max_{X_k, X'_k} \|\mathcal{H}(X_k) - \mathcal{H}(X'_k)\|_2 = \sqrt{|h_1^k - h_1^{k'}|^2} \leq C. \quad (24)$$

□

Then, we define our Gaussian mechanism $\mathbf{G}_{\sigma C} \mathcal{H}$, which output the matrix of noise-perturbed embeddings for X_k :

$$\mathbf{G}_{\sigma C} \mathcal{H}(X_k) = [\tilde{h}_1^k, \dots, \tilde{h}_N^k], \text{ where } \tilde{h}_j^k = \text{Clip}(f(x_j^k, \theta_k), C) + \mathcal{N}(0, \sigma^2 C^2), \forall j \in [N]. \quad (25)$$

Lemma 2. *the Gaussian mechanism with $\mathbf{G}_{\sigma C} \mathcal{H}$ satisfies $(\alpha, \epsilon(\alpha))$ -RDP, where $\epsilon(\alpha) = \alpha/(2\sigma^2)$.*

Proof. The ℓ_2 sensitivity for the function \mathcal{H} is C by Lemma 1. The Gaussian standard deviation for the noise-perturbed embedding is σC , which is proportional to the clipping constant C . Combining it with Theorem 4 yields the conclusion that $\mathbf{G}_{\sigma C} \mathcal{H}$ guarantees $(\alpha, \alpha/(2\sigma^2))$ -RDP. □

In DP versions of our algorithms (i.e., Algorithm 1, 2, 3), at one communication round, we sample a batch of b training instances with indices $\{1', 2', \dots, b'\}$ without replacement, yielding a subsampling ratio $\gamma = b/N$. We define our randomized mechanism with subsampling at one communication round as:

$$\mathbf{G}_{\sigma C} \mathcal{H}(X_k) \circ \text{subsample} = [\tilde{h}_{1'}^k, \dots, \tilde{h}_{b'}^k], \text{ where } \tilde{h}_{j'}^k = \text{Clip}(f(x_{j'}^k, \theta_k), C) + \mathcal{N}(0, \sigma^2 C^2), \forall j' \in [b]. \quad (26)$$

According to Theorem 5, given $\mathbf{G}_{\sigma C} \mathcal{H}$ satisfying RDP, the Gaussian mechanism with subsampling $\mathbf{G}_{\sigma C} \mathcal{H}(X_k) \circ \text{subsample}$ consumes smaller privacy budget due to privacy amplification with subsampling ratio γ . We note that the training process in the server does not access the raw data X_k , thus it does not increase the privacy budget and the whole algorithm in one round satisfies RDP by the post-processing property of RDP. For algorithms with T communication rounds, we use the RDP Composition theorem (Theorem 3) to accumulate the privacy budget over T rounds, and convert the RDP guarantee into DP guarantee (Theorem 2).

Finally, we recall Theorem 1 and provide the formal proof.

Theorem 1. Given a local feature set with N samples, the subsampling ratio $\gamma = b/N$ without replacement, the number of communication rounds T , the clipping threshold C , the noise parameter σ , our DP version of Algorithm 1, 2, 3 satisfies $(Te'(\alpha) + \log \frac{\alpha-1}{\alpha} - \frac{\log \delta + \log \alpha}{\alpha-1}, \delta)$ -DP with $\epsilon(\alpha) = \alpha/(2\sigma^2)$ where,

$$\begin{aligned} \epsilon'(\alpha) \leq & \frac{1}{\alpha-1} \log \left(1 + \gamma^2 \binom{\alpha}{2} \min \left\{ 4 \left(e^{\epsilon(2)} - 1 \right), e^{\epsilon(2)} \min \left\{ 2, \left(e^{\epsilon(\infty)} - 1 \right)^2 \right\} \right\} \right) \\ & + \sum_{j=3}^{\alpha} \gamma^j \binom{\alpha}{j} e^{(j-1)\epsilon(j)} \min \left\{ 2, \left(e^{\epsilon(\infty)} - 1 \right)^j \right\} \end{aligned} \quad (11)$$

Proof. At each communication round, according to Lemma 2, $\mathbf{G}_{\sigma C} \mathcal{H}$ satisfies $(\alpha, \epsilon(\alpha))$ -RDP, where $\epsilon(\alpha) = \alpha/(2\sigma^2)$. Combining it with RDP for subsampled mechanism property in Theorem 4 yields the conclusion that $\mathbf{G}_{\sigma C} \mathcal{H}(X_k) \circ \text{subsample}$ satisfies $(\alpha, \epsilon'(\alpha))$ -RDP. Due to the post-processing property of RDP, our DP algorithms (i.e., DP versions of Algorithm 1, 2, 3) with one round satisfy $(\alpha, \epsilon'(\alpha))$ -RDP. Based on RDP Composition theorem (Theorem 3), our DP algorithms with T communication rounds satisfy $(\alpha, Te'(\alpha))$ -RDP. Based on the connection between RDP and DP in Theorem 2, our DP algorithms with T communication rounds also satisfy $(Te'(\alpha) + \log \frac{\alpha-1}{\alpha} - \frac{\log \delta + \log \alpha}{\alpha-1}, \delta)$ -DP. □

D BROADER IMPACT

Although various algorithms are proposed to improve the model performance in horizontal FL, vertical FL is less studied due to its unique vertically-partitioned data properties and challenges of optimization. This paper presents a novel VFL framework with multiple linear heads (VIM) as well as the ADMM-based method for solving the optimization problem with efficient communication. We provide the differential privacy mechanism for VIM and prove the privacy guarantee. We believe that VIM and the ADMM-based algorithms can benefit the FL community as a standard VFL framework based on our theoretical analyses and empirical results, and promote the development of scalable vertical FL algorithms.

A possible negative societal impact may come from the potential misuse of our work. For instance, directly deploying VFL algorithms without stopping criteria or regularization techniques may lead to the over-fitting phenomenon, as many other algorithms. Based on our experiments, we find that over-fitting is a common problem of VFL algorithms, due to a large number of model parameters from all clients in the whole VFL system. Compared to the centralized learning or horizontal FL, the prediction for one data sample in VFL involves M times model parameters, which corresponds to M partitions of input features. To prevent over-fitting, we use regularizers to constrain the complexity of models and adopt standard stopping criteria, i.e., stop training when the model converges or the validation accuracy starts to drop more than 2%. We have tried our best to define our objective function clearly in Section 3 and state experimental setups in Section 5 to avoid potential misuse of our framework.